Effects of phosphorylation on the ADP-Ribosylation activity of PARP16

Virginia Martín Cristóbal

Degree Project in Biochemistry, 2022
Department of Chemistry
Lund University
Sweden

BSc, 30 hp

LUND
UNIVERSITY

Effects of phosphorylation on the ADP-ribosylation activity of PARP16

Virginia Martín Cristóbal

LUND
UNIVERSITY

Degree Project in biochemistry
2022
BSc, 30 hp

Supervisor:
Herwig Schüler
Lund University
Department of Chemistry
Biochemistry and Structural Biology

Examiner:
Kristine Steen Jensen
Lund University
Department of Chemistry
Biophysical Chemistry

Lund University
Department of Chemistry
Centre for Molecular Protein Science
P.O. Box 124
SE-221 00 Lund, Sweden

Table of Contents

Project summary: Effects of phosphorylation by kinases on the activity of PARP16

This report covers an investigation on protein modification and enzymatic activity. Our protein of interest is known as PARP16/ARTD15 and belongs to a protein superfamily that modifies other proteins by adding ADP-ribose using NAD+ as a substrate (ADP-ribosylation). The proteins from this superfamily are involved in several physiological functions, cell stress responses, and even disease. Therefore, they have been recently identified as important therapeutic targets for cancer and for the modulation of the immune system.

PARPs present various characteristic and essential features in their structure and sequence critical for their ADP-ribosylation activity. In particular, we could highlight their catalytic domain that contains a signature histidine, tyrosine and glutamate (H-Y-E) motif. However, the catalytic domain of PARP16 is composed of H-Y-Y in the catalytic triad and is only capable of performing auto and trans mono-ADP-ribosylation, unlike other PARPs that have poly-ADP-ribosylation activity.

PARP16 has been found to have an important role in the Unfolded Protein Response (UPR) since it is required for activation of two ER stress sensors, PERK and IRE1α. These are so-called kinases and play critical roles in disease development related with protein folding and cancer. Additionally, the same study showed that these two proteins modify PARP16 by adding phosphate residues (phosphorylation).

Aiming to understand this biological mechanism, and due to difficulties to produce PERK and IRE1α, we designed various experiments in which we expressed, purified, and tested several kinases from an Addgene genetic library called ``an open library of human kinase domain constructs for Automated Bacterial expression´´. It contained 72 kinases and 2 phosphatases. The phosphatases are of great relevance because they allow a non-toxic overexpression of the kinases.

The experimentation began with the coexpression of the phosphatases and kinases followed by purification of the kinases with Ni-NTA beads. Next, we tested the autophosphorylation activity and transphosphorylation activity to PARP16 of the kinases in presence of ATP. This showed that the kinases were active and we identified several kinases that phosphorylated PARP16. After the results of both assays, ADP-ribosylation assays were designed in order to investigate

the effects that phosphorylation has on the catalytic activity of PARP16. The results showed a variation of the ADP-ribosylation activity of PARP16. It is remarkable that 2 of the 4 kinases tested in this last assay have the same specificity as PERK and IRE1α and reduce the activity of PARP16.

This discovery can be key to develop therapies to prevent or treat cancer and genetic disease development. However, further investigation is indispensable to elucidate which residues of PARP16 are modified by the kinases and how PERK and IRE1α behave in the presence of PARP16.

Abstract

PARP16/ARTD15 is an intracellular mono-ADP-ribosyltransferase that catalyzes auto- and heteromodification by transfer of a single ADP-ribose moiety. It belongs to the ADP-ribosyltransferase (ART) superfamily. ADP-ribosylation of amino acids on protein targets is critical in the regulation of cellular pathways in eukaryotes, especially involved in physiological functions, cell stress responses and disease. It has been discovered that PARP16 plays an important role in the Unfolded Protein Response (UPR) as the main activator of 2 endoplasmic reticulum (ER) stress sensors, PERK and IRE1α kinases. In addition, it was also found that these kinases phosphorylate PARP16. The aim of this project is to investigate the phosphorylation of PARP16 by the kinases and whether that implies alterations of its activity. To answer this question, we coexpressed Tyrosine-kinases with YopH and Serine/Threonine-kinases with Lambda from an Addgene genetic library. The kinases were purified by a 2-step elution protocol using Ni-NTA beads and imidazole. Although the samples showed signs of phosphatase contamination, we found conditions in which we could assess the phosphorylation activity of the kinases. Finally, phosphorylation and ADP-ribosylation assays were performed with PARP16 and our kinases. The results showed clear phosphorylation of PARP16 and a variation of its ADP-ribosylation activity in the presence of the modification. This discovery opens up new questions about the biological effects that the phosphorylation of PARP16 can have, especially in cancers and protein folding diseases. Therefore, these findings can be critical for therapeutic inhibition and treatment. Further investigation should address questions such as what residues from PARP16 are modified and how phosphorylation by PERK and IRE1α affect the ADP-ribosylation activity of PARP16.

Key words: ADP-ribosylation, Kinases, PARP16, Phosphorylation and UPR.

Acknowledgement

I would like to express my gratitude to Carmen Ebenwaldner for providing me the minipreps from the human kinase domains and the purified PARP16.

Thanks should also go to Herwig Schüler for the opportunity given me to become part of his investigation group and allowing me to do my thesis under his leadership and guidance. Furthermore, for investing in all the reagents and equipment needed to accomplish the main aim of this project, always depositing trust on me which helped me to gain confidence in my work. I would also like to thank my lab group - Carmen Ebenwaldner, Mathieu Long, Archimede Torreta, Constantinos and Antonio García - for all the help provided, the knowledge shared with me and the fun times at the lab together. The help received from them in order for me to learn how to use different equipment and several analysis programs was indispensable. Special mention to Carmen Ebenwaldner for her patience and kindness during this intense and amazing learning period that I have experienced. Ebenwaldner has given me the opportunity to learn and grow in my experiences listed in my thesis, and I have adapted to a more critical and scientific way of learning alongside that.

Many thanks to the Erasmus Scholarship for the generous financial support to travel and study abroad. Also, I am grateful to Lund University, and especially the faculty of Science for accepting my application as an incoming exchange student and my home university for offering the mobility program.

I would also like to thank the unconditional support received from my family and friends. Especially my parents and sister that have always given me emotional and economic support to pursue my dream of becoming a biochemist. I want to also mention my biochemistry friend Sara Trujillo, who was always willing to listen, not only about my lab life and experiments here in Sweden, but also throughout my entire bachelor's degree. I wouldn´t be finishing my degree if it wasn’t because of Sara´s infinite support, and dedication to stick by me through this impactful experience, even in distance. Nonetheless, the new friendships I built were an important factor in helping me succeed at this intimidating, yet honorable experience.

This thesis is dedicated to my mother, Cristina Cristóbal, my biggest inspiration in all aspects of life.

1 Introduction

The ADP-ribosyltransferase (ART) superfamily consists of bacterial pathogenic toxins and eukaryotic ADP-ribosyltransferases [1]. Seventeen poly(ADP-ribose) polymerase (PARP/ARTD) proteins, belonging to the ART superfamily, exist in humans. The primary function of PARPs is to generate ADP-ribose (ADPr) modifications onto target proteins via N-, O-, or S- glycosidic linkages using NAD+ as substrate [2,3]. This modification can occur at many different levels, such as nucleic acid, small molecule or amino-acid modification [3,4]. Our lab is most interested in the latter.

ADP-ribosylation of amino acids on protein targets is critical in the regulation of cellular pathways in eukaryotes and underlies the pathogenicity of certain bacteria. The best understood PARP roles include physiological functions in cell division, transcriptional regulation and regulation of protein degradation, but also cell stress responses such as DNA damage, heat shock, and ER stress response [5]. Several members of the ART superfamily are highly relevant for disease; these include the poly(ADP-ribose) polymerases (PARPs), recently identified as important therapeutic targets for cancer and for the modulation of the immune system [3].

The PARP catalytic domain contains a signature histidine, tyrosine and glutamate (H-Y-E) motif originally identified in various bacterial mono-ADP-ribosyltransferase (mART) toxins. Based primarily on the presence of this triad, ARTs are classified as poly-ADPr synthesizing, mono-ADP-ribose (mADPr) synthesizing, or enzymatically inactive [1,5,6]. Many of these PARP-like proteins are unlikely to carry out genuine ADP-ribose polymer formation due to the lack of the catalytic glutamate residue critical for polymerase activity. In addition, secondary structural features of the PARP catalytic domain, such as the Donor loop (D-loop) and the acceptor pocket, are also predicted to influence catalytic activity [5].

Human PARP16/ARTD15 is a 36-kDa intracellular mono-ADP-ribosyltransferase that catalyzes auto- and heteromodification by transfer of a single ADP-ribose moiety [1,5]. An additional feature of ARTD15 is that it is the only ARTD family member with a carboxy-terminal transmembrane domain, necessary and sufficient for its localization to ER membranes. The amino-terminal cytosolic catalytic domain possesses the amino acids H-Y-Y in the catalytic triad [4].

This ER transmembrane protein has been found to have an important role in the Unfolded Protein Response (UPR) [8]. The enzymatic activity of PARP16 is up-regulated during ER stress response when it (ADP-ribosyl)ates itself, PERK and IRE1α. These two kinases, PERK and IRE1α, are 2 of the 3 proteins that function as ER stress sensors. However, their ADP-ribosylation by PARP16 is sufficient for activating them in the absence of ER stress [7,8]. Modification of PERK and IRE1α by PARP16 increases their kinase activities and the endonuclease activity of IRE1α [7].

Furthermore, PARP16 phosphorylation was observed in the same study, suggesting that PARP16 is likely a substrate of PERK and IRE1α. Phosphorylation by PERK was detected to be NAD+ dose-dependent, whereas IRE1α phosphorylation does not appear to be NAD+ concentration-dependent [7].

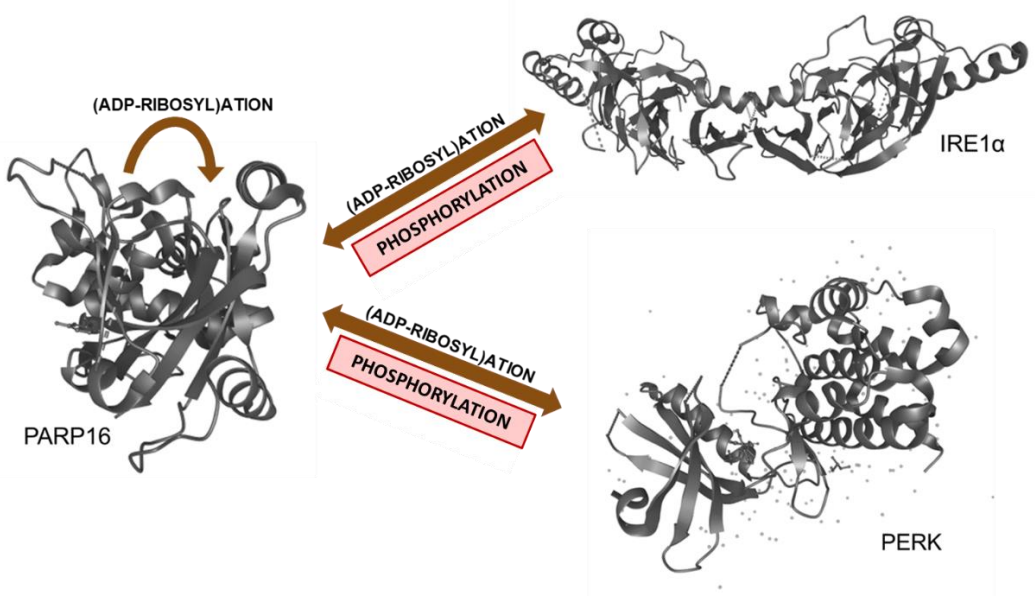

Figure 1: Scheme of the interactions between PARP16/ARTD15, PERK and IRE1α

Since kinases play a critical role in cellular signaling and are dysregulated in a number of diseases, such as cancer, diabetes, and neurodegeneration, this finding can be critical for therapeutic inhibition for cancers and protein folding diseases, such us Parkinson's disease, Huntington's disease, and Alzheimer's disease [9,10].

The aim of this thesis was to investigate whether phosphorylation on PARP16 can alter its ADP-ribosylation activity *in vitro*. Therefore, we bought ``an open library of human kinase domain

constructs for Automated Bacterial expression´´, a library of 72 His-tagged human kinase domain constructs intended for phosphatase coexpression [9]. The library contains 10 Tyr-specific-kinases intended for co-expression with the Tyr-specific YopH phosphatase and 62 Ser/Thr-specific-kinases compatible with the Ser/Thr-specific Lambda phosphatase. This approach is thought to reduce toxicity and hereby increase the yield in the expression system, *E. coli*. Our intention is to express and purify them, test their activity, and elucidate the possible phosphorylation of PARP16 and its effects on the ADP-ribosylation activity of PARP16.

2 Materials and Methods

Minipreps of Kinase Library from Addgene – Background and plasmid filing

The plasmid library was ordered from Addgene (Kit #1000000094). To begin the work with its content we performed minipreps of all plasmids provided. The miniprep kit used was Gen Elute Plasmid Miniprep Kit (1003311632). Only few changes were made to the manufacturer´s protocol described in the kit: we centrifuged at 14,8 rpm and we used 50 µl of molecular biology reagent water for plasmid elution. The concentration of the plasmid samples was determined based on absorbance measurements at 260 nm with the Nanodrop and they were stored at -20ºC.

Cotransformation

As stated by Albanese SK et al., the Addgene library was designed to allow fast and nontoxic expression of human kinase domain constructs when the phosphatases were coexpressed with the kinases [9]. According to those statements, we cotransformed chemically competent cells with kinase plasmids and their respective phosphatases. The cells used were pRARE3 cells provided by my lab coworkers.

The setting of the experiment was based on the compatibility between kinase domains and the phosphatases. The cells were cotransformed by a heat shock protocol by subsequently adding 1 µl of each plasmid to 20 µl of competent cells and then recovered with SOC out broth medium from BIOlabs (B9020S). The contransformed cells were plated in ampicillin and streptomycin resistance LB-agar plates and incubated at 37ºC overnight.

Medium-scale expression test and purification of Lambda and YopH coupled kinases

1ml LB cultures, supplemented with ampicillin and streptomycin, were inoculated with single colonies from the double-resistance plates. Turbidity by ocular inspection was used as an indicator of cell growth. The cultures were incubated 2-3 hours at 37ºC and 210 rpm.

Aiming to increase the yield of our expressed proteins, we moved onto medium scale cultures by preparing 50 ml LB broth media with 50 µl of ampicillin and 50 µl of streptomycin, and adding the 1 ml culture once it had reached a high turbidity. Cell growth was determined by optic density at 600 nm (OD600). The target OD600 was approximately 2 to begin with the induction. The cultures were prepared in 250 ml Erlenmeyer and incubated for 4 hours at 37ºC

while being shaken at 210 rpm. 100 mM IPTG was the induction agent used for overnight induction at 18ºC and 210 rpm. Next, cells were centrifuged at 12000 rcf, and the pellets were lysed by adding 200 µl of Lysis buffer full (50mM Hepes pH 7,5, 500mM NaCl, 0,5 mM TCEP, 10% glycerol, 50% B-Per, 10% Protease Inhibitor cocktail and 110mM/10 ml of DNAse). The lysates were then transferred to Eppendorf tubes and frozen at −80 °C overnight.

For protein purification, 3 methods were tried for optimization: **1)** We used 60 µl of 1:1 NI-NTA Agarose bead suspension from QIAGEN (1000632) equilibrated in lysis buffer. The lysate was thawed and clarified by centrifugation; therefore, the supernatant could be transferred to the Eppendorf tubes containing the equilibrated beads. The pellet was resuspended in 200 µl of lysis buffer and saved. The Eppendorf tubes were incubated at 4ºC in a swinger for 2h. After that, we spun them down at 4ºC and 500 rfc for 5 min, saved the supernatant (unbound) and resuspended the beads with 1 ml of lysis buffer. We spun them down under the same conditions, discarded the supernatant, resuspended the beads in 1 ml lysis buffer and spun one more time at the same conditions. We discarded the supernatant, added 8 µl Laemmli buffer directly to the beads and boiled them at 95ºC (elution/bound). After this protocol we had 3 samples per protein tested: pellet (p), unbound (u) and elution (e); **2)** We equilibrated 400 µl Ni-NTA bead suspension. The lysate clarification was performed by freezing and thawing the lysates with liquid nitrogen and spinning it down at 10000 rfc for 15 min. We took an aliquot of the SN (for SDS-Page analysis) and transferred the lysate to the beads into 15 ml falcons and let them incubate for 2h. The pellet was resuspended in 2 ml of lysis buffer and saved. After 2-hour incubation, we spun down the lysates with the beads, took an aliquot of the SN (unbound), removed the rest and resuspended the beads. Then, we transferred them to Bio-Spin Chromatography columns from BIORAD (7326207), washed them 3 times with lysis buffer, discarded the last wash and left it incubating overnight with 0,2 mg/ml of TEV protease in lysis buffer at 4ºC shacking. This step was added to elute the proteins because there is a TEV cleavage site between the His-Tag and the kinase domains, and avoid the use of imidazole. Next, the flow-through was saved and columns were washed twice with lysis buffer. We took an aliquot from the flow-through (e1). After that we eluted the rest of the proteins bound to the beads by using an elution buffer containing 50mM of HEPES pH 7´5, 300mM of NaCl, 10% glycerol, 400mM imidazole and 0´5mM TCEP. The eluate was saved (elution 2 = e2). This protocol left us with 5 samples per protein tested: pellet (p), supernatant (SN), unbound (u), elution 1 (e1) and elution 2 (e2); **3)** The protocol followed is very similar to

the second one but the TEV cleavage was replaced with a two-step elution with different imidazole concentrations. Imidazole is key due to its ability to compete with the His-Tag for binding to the beads because the structures are very similar. After incubation of the NI-NTA beads with the lysate, we spun down the beads, saved an aliquot of the SN (unbound), removed the rest and resuspended the beads. We transferred the beads to the Bio-Spin Chromatography columns, washed them 3 times with lysis buffer, removed the last wash and directly eluted with 500 µl of elution buffer 1 containing 50mM Hepes pH 7,5, 300mM NaCl, 0,5 mM TCEP, 10% glycerol and 50mM imidazole and saved the flow through (e1). Then eluted with 500 µl of elution buffer 2 containing 50mM Hepes pH 7´5, 300M NaCl, 0,5 mM TCEP, 10% glycerol and 400mM imidazole and saved the flow through (e2). The samples saved from this protocol are equivalent to the ones in protocol number 2.

The samples saved for SDS-PAGE were prepared for the gel electrophoresis by adding 10 µl of the saved sample and 5 µl of SDS-sample buffer (Laemmli buffer). The pellet sample had to be diluted by adding 10 µl of water to avoid problems while loading the gel. All the samples were boiled at 95ºC for 4 min and then loaded. We ran Invitrogen Nu-Page 4-12% gels (10-17 wells) for 35 min at 200 volt and 120 mA. The ladder used was SeeBlue plus2 prestained standard (1x) from Invitrogen and the staining reagent was homemade Yasumitsu staining (PMID: 20599644) (20% citric acid, 0,05% Coomassie blue g250 and 25% pvp-40).

Auto-phosphorylation activity assay with selected kinases

Once we had our kinases isolated, we tested their activity. The aim of our first assay was to determine whether the domains had auto-phosphorylation activity. We used western blotting with phospho-specific antibodies to design the experiment.

The reaction set up was divided in two, because we also tested two different reaction buffers. The reactions buffer used were: Reaction buffer A (10x): 500mM HEPES 7.5, 1M NaCl, 10mM MgCl2, 1mM TCEP and reaction buffer B (10x): 500mM Na2HPO4 pH 7.5, 1M NaCl, 10mM MgCl2 and 1mM TCEP. Buffer B required to add MgCl2 individually, otherwise it would precipitate in the 10x buffer. MgCl is of great importance because most kinases need magnesium for activity. We prepared 20 µl aliquots and incubated them for 1 h at 37 ºC. The aliquots contained 4-10 µM of Kinase, 200 µM of ATP, 2 µl of 1x Buffer and 2 µl of phosSTOP EASYpack from ROCHE (ref: 04906845001). The phosSTOP EASYpack was prepared by dissolving 1 tablet in 1 ml of miliQ water. The selection of the kinases used for this experiment

was based on Uniprot´s information about its auto-modification activity and its yield after purification. We selected 3 Tyrosine specific kinases (EPHB3, EPHB2, FGFR1) and 3 Threonine/Serine specific kinases (KCC2D, STK24, GAK). Reaction tables can be found in the appendix [Figure A2 and A3]. We stopped the reactions by adding 8 µl SDS-sample buffer and boiling them at 95ºC for 2 min. Samples were loaded to Invitrogen Nu-Page 4-12% gels (10-17 wells).

For the wet transfer, we prepare transfer buffer (0,03% (w/v) Trizma, 0,144% (w/v) Glycine and 10% (v/v) methanol). We used PVDF membranes activated in 100% methanol for a few seconds. The gel and membrane were soaked in the transfer buffer for 10min. We used the Invitrogen chamber System using two properly soaked sponges and two filter papers on each site. The electroblotting was performed by running the NuPage Blot program: 60min, 25V, 17W, 160mA. After transfer, the membranes were stained with Ponceau S solution for 5min, washed with water and imaged. TBST was used for distaining for 5 min and then the membranes were blocked with 1% BSA in TBS-T for 25 min.

The primary antibodies (AB) used, Anti-p-Thr Antibody (H-2): sc-5267, Anti-p-Tyr Antibody (PY99): sc-7020 and Anti-p-Ser/Phosphoserine Antibody (16B4): sc-81514, were bought from Santa Cruz Biotechnology. We diluted them 1:200 in TBS-T with 1% BSA following the provider protocol to a final volume of 10 ml. The membranes were placed in sealed bags with the AB and incubated the membrane overnight at 4ºC shacking. After washing 3 times for 5-10 minutes the membranes were incubated with a dilution 1:5000 of HRP-fused Anti-Mouse IgG (H+L) (Invitrogen 62-6520) in TBST- 1% BSA according to the provider´s recommendation. Again, the membranes were placed in sealed bags with the AB and incubated the membrane at room temperature for 1 hour. For membrane development we used SuperSignal West Pico PLUS Chemiluminescent Substrate (ref 34577) from Bio-Rad in a 1:1 dilution and imaged the membranes using BIORAD ChemiDoc Imaging System.

Trans-phosphorylation activity assay with selected kinases and PARP16

The principle of the assay is the same as in the auto-phosphorylation assay described above. The protocol is based on western blotting and activity detection by using primary and secondary antibodies. Although, the reaction set up differed. We perform this assay only using Reaction buffer A, since no major differences were found in the previous experiment. The 20 µl aliquots contained 10 mM of PARP16 in addition to everything stated in the previous experiment. In

this case, the assay was performed with 5 Tyr kinases (EPHB3, EPHB2, FGFR1, ABL1 and CSK) and 7 Thr/Ser kinases (KCC2D, STK24, GAK, KCC1G, CDK16, HASP and PMTY1). We also set up 2 controls for each reaction: 1) with 200 mM EDTA and no ATP as a negative control; 2) with ATP but no PARP16 as a positive control. The reactions were incubated for 2 hours at 37ºC and 210 rpm, then stopped with 8 µl of SDS-sample buffer and boiled for 2 min at 95ºC. Samples were stored at -20ºC. Reaction tables can be found in the appendix [Figure A4 and A5].

The samples were run in the BIORAD Stain Free SDS-PAGE gel system and we used its specific ladders, Precision Plus All Protein ladder and Precision Plus Protein Western C ladder. The Western Blot procedure was followed as for the auto-modification assay.

We used Image Lab Software for membrane and gel quantification. Every time the PARP16 control was used as reference and we normalized the data against the loading control. The results obtained were plotted in excel.

ADP-ribosylation activity assay with selected kinases and PARP16

Lastly, we designed an experiment to determine PARP16 activity over time and the effects of the potential pre-phosphorylation by selected kinases. Again, the method used is Western Blotting, however, for this assay we used Streptavidin-HRP which is not an antibody but a protein that binds strongly and specifically to biotin. We added biotin-NAD that will produce biotin-ADPr which can then be detected by Strep-HRP. The reaction set up was more complex than previous experiments. Firstly, we prepared phosphorylation reactions containing 10 µM PARP16, 3-4 µM Kinase and 200 µM ATP. These reactions were incubated at 37ºC and 210 rpm for 30 min. Meanwhile, we prepared a 100 µl reaction only containing 10 µM PARP16. After the incubation period, we set up ADP-ribosylation reactions by adding 200 µM of NAD-mix containing 10% biotin-NAD+ in NAD+ and incubating the reactions at 37ºC and 210 rpm for 4 hours. Throughout that time, we took 20 µl aliquots from the PARP16 reaction at different time points (0, 0,5, 1, 2, 3 and 4 hours). The reactions were stopped with 8 µl of SDS-sample buffer and boiled for 2 min at 95ºC after 4hours

The Western Blot was performed using the BIORAD Stain Free SDS-PAGE gel system and we used its specific ladders, Precision Plus All Protein ladder and Precision Plus Protein Western C ladder. The gels were run for 45 min at 200 volt and 120 mA. The protocol, after that, was

identical to the two previous assays, until incubation with primary AB. In this case the membranes were incubated for 1 hour with 0,5 mg/ml Streptavidin- HPR in 1%BSA in TBST. Membrane development was performed with SuperSignal West Pico PLUS Chemiluminescent Substrate (ref 34577) from Bio-Rad in a 1:1 dilution and the membrane imaging by using BIORAD ChemiDoc Imaging System.

We used Image Lab Software for membrane and gel quantification. Every time the PARP16 control at time point 0 was used as reference and we normalize the data against the loading control. The results obtained were plotted in excel.

3 Results and discussions

Successful transformation of pRARE3 competent cells

There are different ways to transform competent cells. We opted for a co-transformation protocol, aiming for a fast and effective method to obtain transformants. We used double resistance plates to ensure that our transformants would co-express, as earlier stated, the kinases and phosphatases. This step was critical since the kinases and phosphatases are encoded on different plasmids. Once we optimized the protocol, we found the co-transformation to be successful and reproducible. Plates had between 2 and over 100 transformants after overnight incubation at 37ºC.

Kinase expression and purification tests show signs of phosphatase contamination

After inducting with IPTG and spinning down the cells, the pellets were weighted to determine the cellular mass. The pellets were in a range of 0,8-1 g, which were the results expected according to the amount of culture incubated (50ml).

The purification of the kinases began after lysing the cells. Our aim was to obtain the protein of interest in a soluble, active and pure state. Initially, we tried a protein isolation procedure based only on the affinity of the His-Tag attached to the kinases to the Ni-NTA beads. The principle of this method was to incubate the soluble fraction with Ni-NTA beads, wash off the unbound proteins and elute the His-tagged kinases. This elution step was performed by adding Laemmli buffer and boiling at 95ºC. Applying this protocol, we tested 10 YopH compatible Tyr-Kinases. However, the gel analysis showed that all tested kinases are insoluble as the corresponding overexpression bands can be found in the pellet aliquot [figure 2]. To determine whether the bands corresponded to our kinases, we used Uniprot and Expasy to calculate the approximate molecular weight of each construct. It is important to point out that in figure 2B it is possible to see overexpressed bands also in the elution aliquot for CSK. Considering all the results, we concluded that we needed to optimize the lysis procedure. Also, we can already see that YopH has a very similar molecular weight to the kinases, which will add complexity to the result analysis.

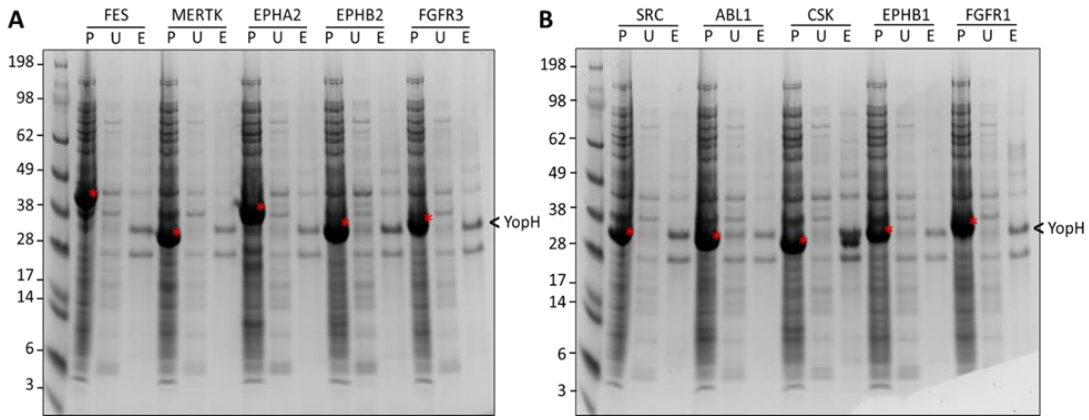

Figure 2: Purification of YopH compatible kinases using NI-NTA beads and elution with Laemmli buffer. A) SDS-PAGE gel from FES, MERTK, EPHA3, EPHB2 and FGFR3. B) SDS-PAGE gel from SRC, ABL1, CSK, EPHB1 and FGFR1. P (pellet), U (Unbound) and E (elution). In both images the red asterisk corresponds to the overexpressed band. YopH molecular weight is pointed out with a black arrow.

Since an overexpression band was seen for CSK in the elution aliquot, we used this protein for the following experiment. We designed a second protocol aiming to optimize and avoid the issues encountered earlier. In this case, we slightly altered the contents of the lysis buffer in order to obtain proper lysates and we tried to isolate the kinase from the phosphatase at the plating stage. To isolate the phosphatase, we cotransformed pRARE3 cells with the plasmid containing YopH and incubated it in single resistance plates. This experiment was designed to determine whether the purified kinases were contaminated by YopH, as we did not know the exact mobility shift in gel electrophoresis. Therefore, we tested CSK and CSK+YopH in parallel. Also, a few changes were made to the purification protocol. We added a TEV-Cleavage step and the final elution was done with a buffer containing imidazole. This step was implemented because we could asses phosphatase contamination in figure 3 and according to the Albanese at al [9], cleavage with TEV protease minimized phosphatase contamination in the resulting eluate because it does not cause the elution of phosphatases due to their substantial affinity for the nickel beads. The SDS-PAGE gel was imaged and it was possible to observe overexpression bands corresponding to the S (supernatant), U (Unbound), and e2 (elution 2) fractions, 3 of the 4 soluble fractions loaded [Figure 3]. The cleavage with TEV was not successful and instead the overexpressed protein eluted with the addition of imidazole in elution 2 (e2). Although, the samples did not appear to have many differences in the bands, when theoretically we expected to have different protein contents after plate isolation of CSK. In

addition, the molecular weights of YopH and CSK are very similar therefore we see overlapping bands which complicate the analysis of the results.

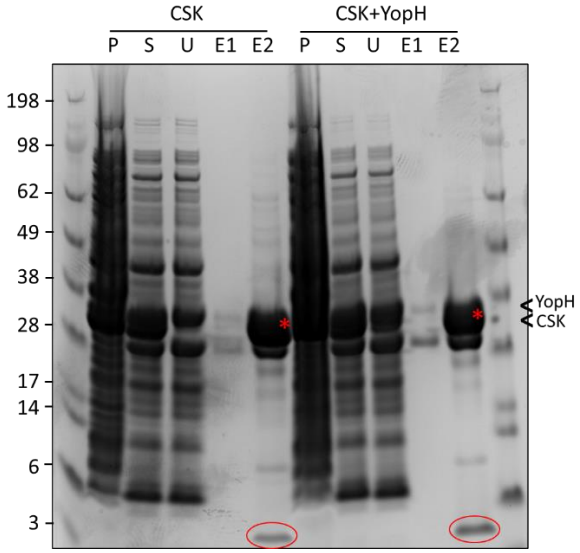

Figure 3: Purification of CSK and CSK + YopH through the TEV cleaveage and 1 elution step method. P (pellet), S (supernatant), U (Unbound), E1 (elution 1; TEV-cleavage) and E2 (elution 2; imidazole). The red asterisk corresponds to the most intense overexpression band of each sample. The molecular weights of YopH and CSK are pointed out with a black arrow. The cleaved His-Tag is marked with a red circle.

After all, the TEV-cleavage protocol did not result in uncontaminated kinase eluate which was our main aim to then proceed onto activity assays. Therefore, we developed a purification method based on a 2-step elution protocol using 2 buffers with an increasing concentration of imidazole. For this experiment we used 4 of the previously tested Tyr-kinases: EPHA3, EPHB2, ABL1, FGFR1. Figures 4A and 4B show the purification results of this method. The proteins were overexpressed in a soluble state and were eluted at the lowest concentration of imidazole. Yet, we could observe a double band for this aliquot which indicated phosphatase contamination of the sample. In order to determine if that band corresponded to YopH, another gel was run with a new purified sample of YopH, that was obtained following the 2-step elution protocol, and elution 1 from each purified kinase [Figure 4C]. As predicted, based on the mobility shift in SDS-Page, we concluded that the second band belonged to YopH. These results were very important and to be taken into account for the following activity assays performed.

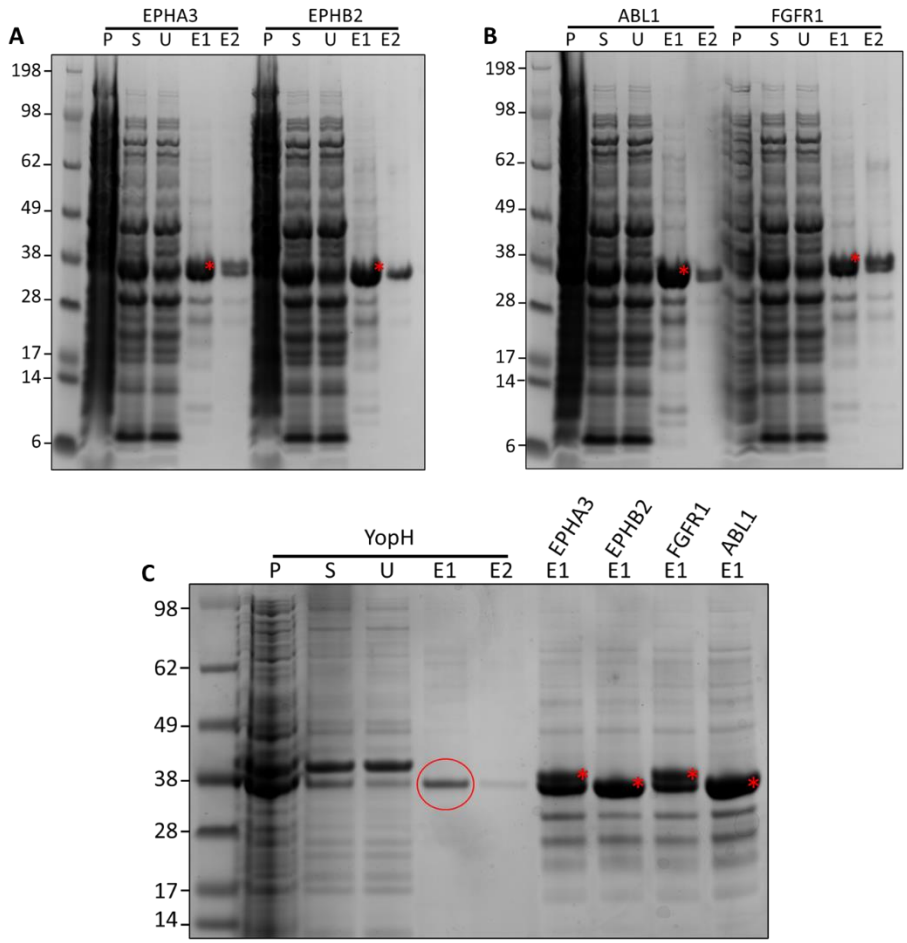

Figure 4: 2 step elution purification protocol of 4 YopH compatible kinases: EPHA3, EPHB2, ABL1 and FGFR1. A) SDS-PAGE gel from EPHA3 and EPHB2. B) SDS-PAGE gel from ABL1 and FGFR1. C) SDS-PAGE gel from YopH purification compared with the fraction e1 from the 4 tested kinases. P (pellet), S (supernatant), U (Unbound), E1 (elution 1, conc. imidazole) and E2 (elution 2, conc. imidazole). The red asterisk corresponds to every kinase overexpression band. The red circle marks the YopH overexpression band.

The plasmid library also contained another set of coupled phosphatases and kinases, the Lambda compatible Ser/Thr- kinases, which were also expressed and purified. Since we had already optimized the purification protocol, we only performed the 2-step elution purification protocol. The results displayed in figure 5 were very similar to the ones obtained for the previous kinases. We could observe overexpression bands in soluble state, all corresponding to e1, but still signs of phosphatase contamination. In this case it is remarkable that the molecular weight of Lambda differs greatly from its compatible kinases, which made it easier to analyze the results. Also, we could asses a lower band intensity which indicates a lower protein yield. This is important for the reaction set up in the future activity assays.

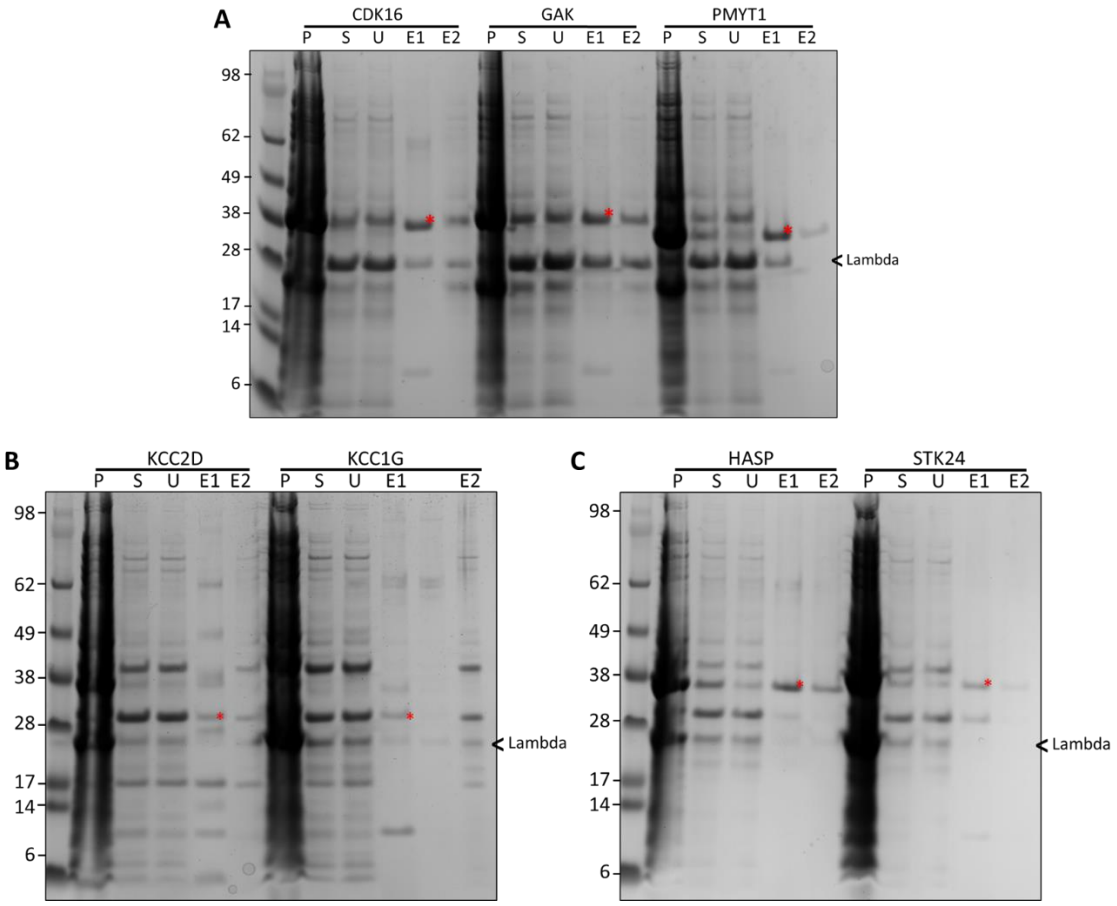

Figure 5: 2 step elution purification protocol of 8 Lambda compatible kinases: CDK16, GAK, PMYT1, KCC2D, KCC1G, HASP and STK24. A) SDS-PAGE gel from CDK16, GAK and PMYT. B) SDS-PAGE gel from, KCC2D and KCC1G. C) SDS-PAGE gel from HASP and STK24. P (pellet), S (supernatant), U (Unbound), E1 (elution 1, conc. imidazole) and E2 (elution 2, conc. imidazole). The red asterisk corresponds to every kinase overexpression band. The molecular weight of Lambda is pointed out with a black arrow.

Selected kinases display automodification activity

Before testing the trans-modification of PARP16 by the kinases, we wanted to assess their kinase activity via auto-modification experiments, and optimize the read-out conditions for phosphorylation activity. In order to design the assays, we researched in Uniprot database which of them had autophosphorylation activity. According to that information and the concentration of our sample we selected 3 Tyr-kinases and 3 Ser/Thr-kinases to test their automodification activity. The selected kinases were EPHA3, EPHB2, FGR1, KCC2D, STK24 and GAK. Each kinase was tested twice with a different buffer to determine optimal activity conditions. We loaded the reactions on gels, performed western blotting and visualized specific

phosphorylation with specific antibodies. The developed membranes are shown in figure 6 next to its corresponding SDS-PAGE gel image.

Tyr-kinases, as previously mentioned, had a higher concentration which allowed us to use 10µM kinase per reaction whereas for the Ser/Thr- kinases we had to use only 4µM, except for GAK that we were able to use 10µM. This is significant when comparing the band intensity of the gel and membranes due to the commensurability between concentration and activity. In figure 6A we can see that there is a great specificity of the Tyr-Kinases and its primary antibody, allowing a clear identification of automodification activity of the proteins. All of the 3 kinases display autophosphorylation activity with EPHA3 being the one with the lowest activity. On the other hand, figure 6B corresponds to Ser/Thr- kinases gel and membranes. To determine the activity of these proteins and the antibody specificity we incubated the membrane with 2 different phospho-specific primary antibodies: p-Thr and p-Ser. Although the antibodies have specificity towards phosphorylation, this assay showed that the automodification activity can only be determined when using the p-Ser antibody. These results suggest that our kinases only phosphorylate serine residues. The 3 proteins tested displayed activity, however GAK presents a single activity band when using p-Thr AB and a double activity band when using p-Ser AB, which is not well understood. One explanation could be that GAK is also able to phosphorylate the serines and threonines in Lambda and, since the samples were contaminated, we can detect activity at the molecular weight of Lambda.

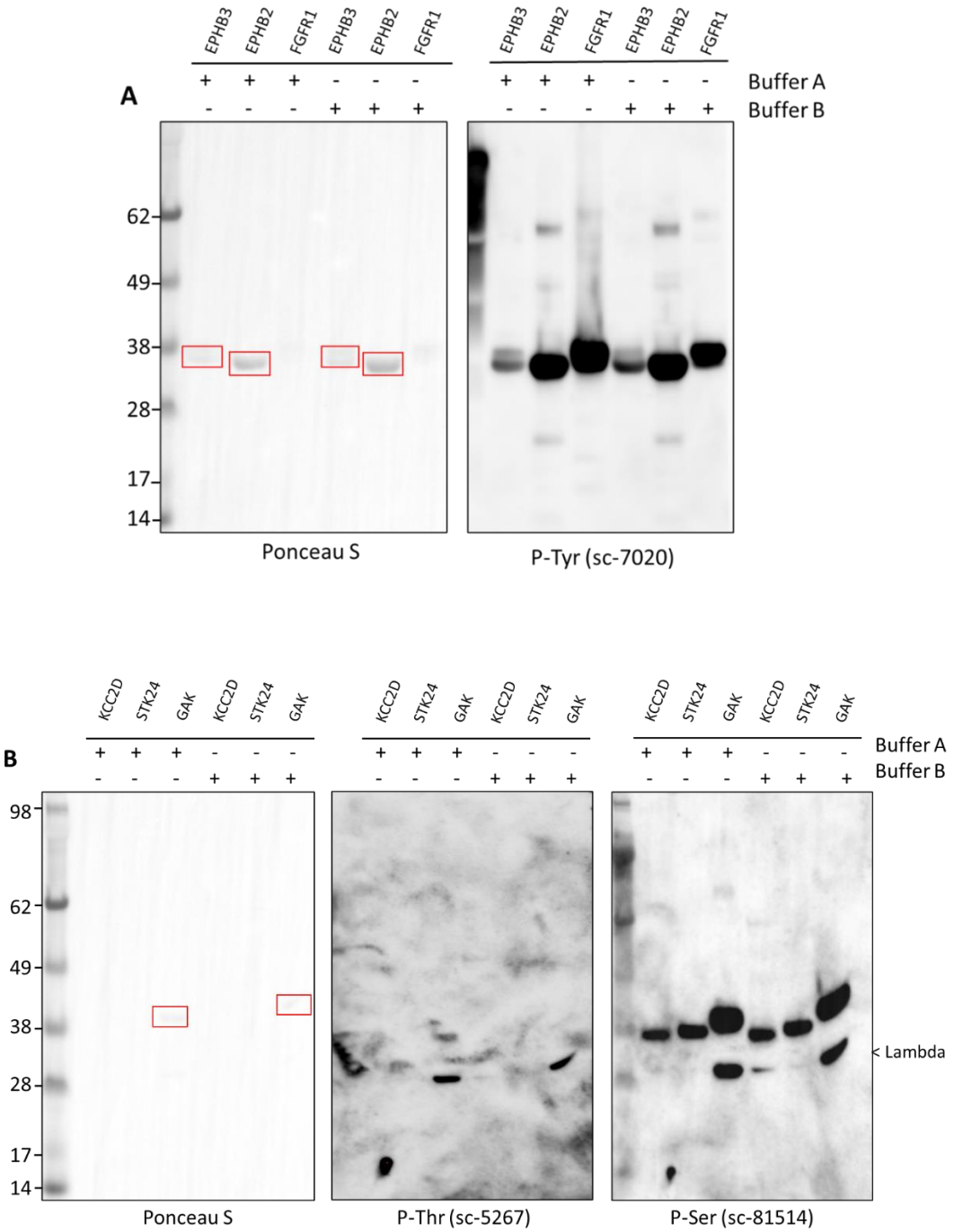

Figure 6: Automodification assay of the purified kinases and antibody specificity determination. A) Ponceau-stained and developed membrane from Tyr-Kinases. B) Ponceau-stained and developed membrane from Ser/Thr-Kinases. The ladder used was SeeBlue Prestained from Invitrogen. The red boxes identify the visible bands in the imaged gels. The primary antibody used is written down underneath each developed membrane.

To test whether putative phosphatase activities were inhibited in the presence of phosphate ions, we compared reaction conditions by using two buffers: a phosphate buffer and a Hepes buffer. Nevertheless, the results of the reactions in presence or absence of phosphate did not vary. Therefore, for simplicity we designed the remaining phosphorylation assays using the Hepes buffer.

PARP16 is phosphorylated by selected kinases

Once autophosphorylation activity had been positively tested, we started investigating whether our selected kinases could also phosphorylate our target protein, PARP16. Experiments were run for both Tyr-kinases and Ser/Thr-kinases. Nonetheless, we only have conclusive and proper results for Ser/Thr-Kinases due to issues with gel running and membrane development with the other kinases.

The activity signals detected in the membranes differed from our initial predictions. Based on previous knowledge and research we expected to detect activity only from the samples containing kinase, PARP16 and ATP and the sample containing kinase and ATP of each of the 7 tested kinases [Figure 7]. Instead, we found phosphorylation in every sample in which PARP16 was present: PARP16 control, PARP16+kinase+ATP and PARP16+kinase+EDTA. The highest intensity band always corresponded to PARP16 molecular weight indicating that it had been phosphorylated. These results suggest that the sample of PARP16 worked with has a previous phosphorylation in its molecule prior to our phosphorylation assay. Probably it was phosphorylated during expression in *E. coli*. Another possible explanation is that the antibodies worked with also present specificity towards PARP16.

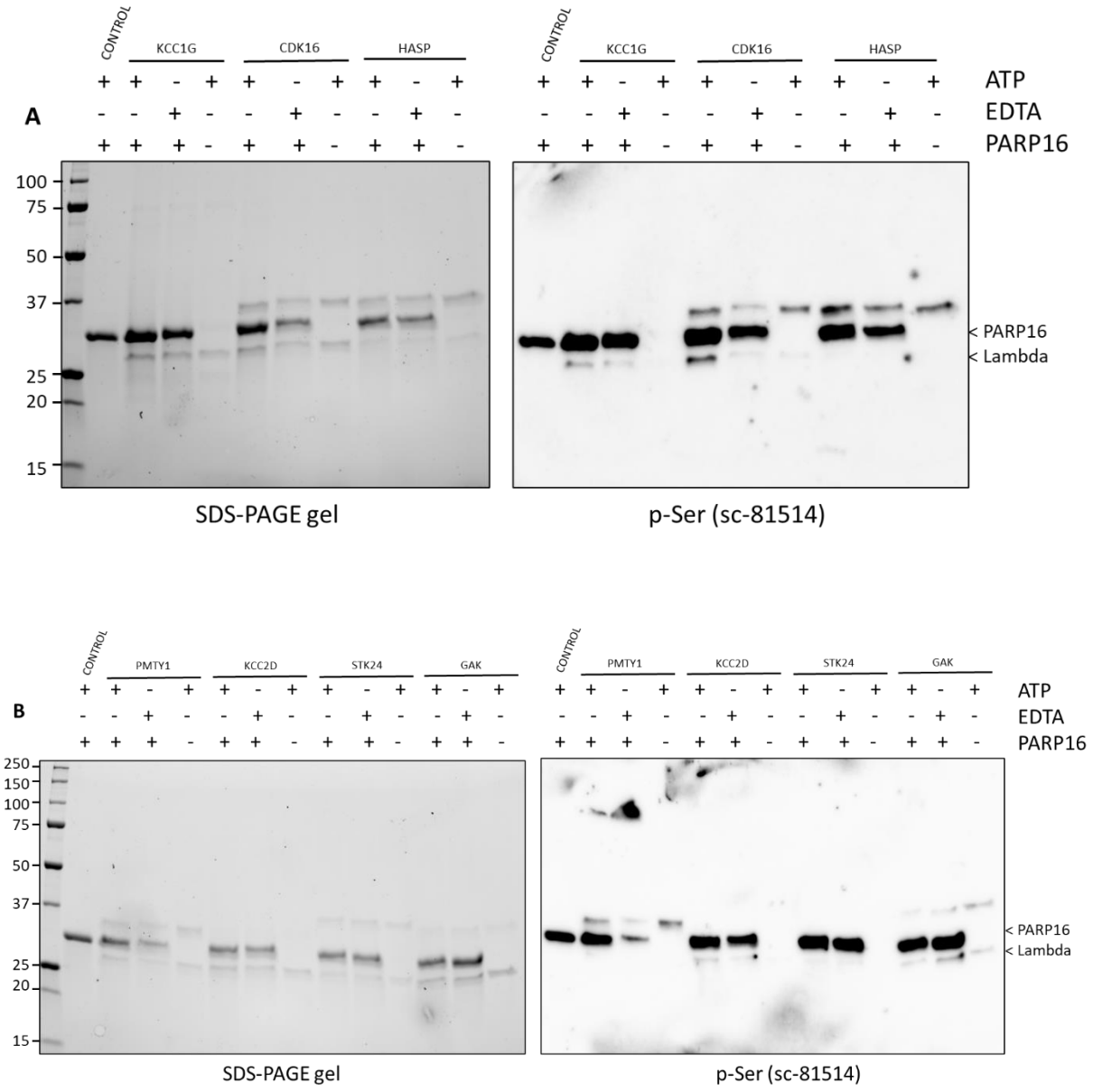

Figure 7: Activity assay of the Lambda compatible kinases on PARP16. A) SDS-PAGE gel and developed membranes from KCC2D, STK24 and GAK. B) SDS-PAGE gel and developed membranes from KCC1G, CDK16, HASP and PMTY1. The gels are Stain free from BIORAD and the ladder is the Precision Plus All Protein ladder. Sample content: P = PAR16+ATP; A = kinase + P16 + ATP; B= kinase + P16 + EDTA; and C = kinase + ATP.

To determine whether our selected kinases phosphorylate PARP16 in vitro, in addition to possible pre-phosphorylation, we used Image Lab software to quantify the relative intensity of each band using the PARP16+ATP band as reference. We did this procedure with each membrane to normalize it according to the loading control. We compared the band intensity from the samples containing PARP16+kinase+ATP and PARP16+kinase+EDTA. Figure 8 shows the data represented in a column graph.

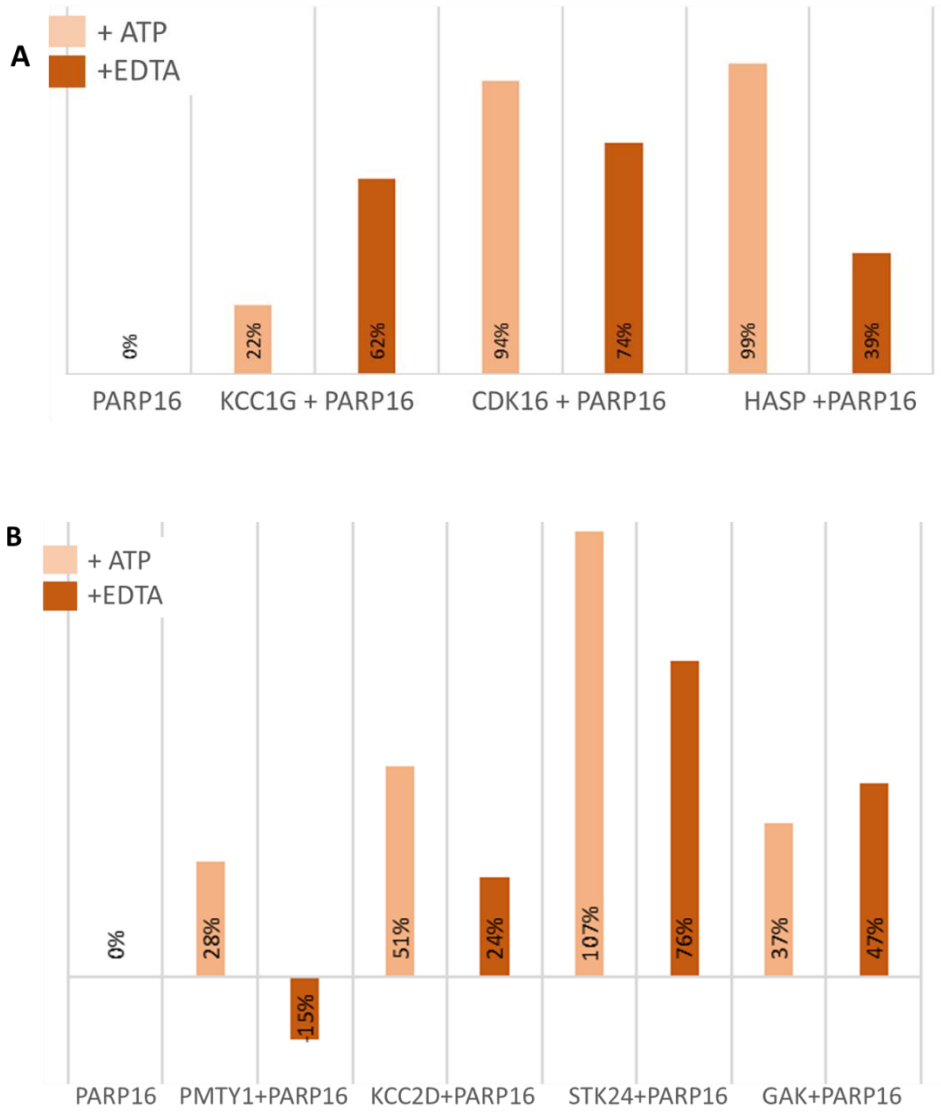

Figure 8: Quantification and normalization of the activity assay of the Lambda compatible kinases on PARP16 using Image Lab Software. The sample containing PARP16 and ATP was used as reference. A) Quantification of the SDS-PAGE gel and developed membranes from KCC2D, STK24 and GAK. B) Quantification of the SDS-PAGE gel and developed membranes from KCC1G, CDK16, HASP and PMTY1.

After analyzing the normalized relative values, we can observe an increasing tendency on the phosphorylation activity when ATP is added to the reaction. But the results are inconsistent and inconclusive, as in some kinases the trend is reversed. In general, more residues of our target protein are modified when kinases and ATP are present because one of the phosphates of ATP is transferred by the kinase to PARP16 during phosphorylation.

Phosphorylation of PARP16 has a direct effect on its ADP-Ribosylation activity

The purpose of designing this assay was to, after all, investigate the evolution of the ADP-ribosylation activity of PARP16 in a period of 4 hours and how the presence of selected kinases affects it. We compare the ADP-ribosylation activity of different samples of PARP16 incubated with and without kinases and induced with a mixture of 10% biotin-NAD in NAD. The experiment set up consisted of an initial 30 min incubation of PARP16 with the kinases in a phosphate buffer with ATP. This step allowed the kinases to phosphorylate PARP16 in order to see if this modification affects the activity of PARP16. In parallel, we prepared a sample containing PARP16 without ATP or kinases. Next, we added NAD mix to each sample and incubated them for 4 hours. In the meantime, we took aliquots from the reaction containing PARP16 without kinases at different time points to see the evolution of the ADP-ribosylation. After 4 hours, all the reactions were stopped by adding Laemmli buffer and heating at 95ºC. We loaded the reactions on gels, performed western blotting and visualized the ADP-ribosylation with Streptavidin-HRP.

In figure 9 we can clearly see that all of the samples present ADP-ribosylation activity. The aliquots from the time point obtained from the reaction containing PARP16 without kinases seem to follow an increasing tendency of activity with time. On the other hand, when PARP16 was previously incubated with the kinases we can appreciate alterations on the ADP-ribosylation activity. For further analysis of the intensity variation of the bands a quantification analysis was required. In addition, this assay was replicated to reassure the veracity of the data extracted from it.

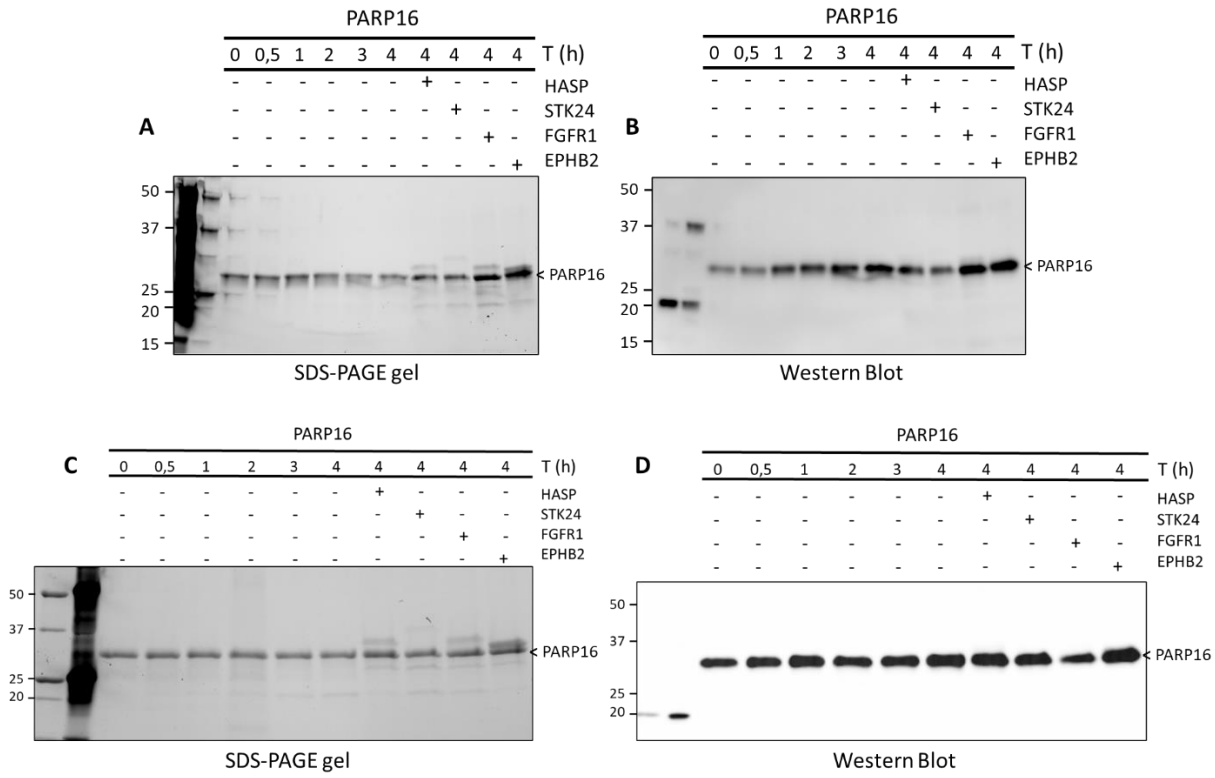

Figure 9: ADP-ribosylation assay of PARP16 without kinases over time and incubated with kinases at time point 4 hours. A) SDS-PAGE gel before transfer from the first assay. B) Developed membrane from the first assay. C) SDS-PAGE gel before transfer from the second assay. D) Developed membrane from the second assay. The gels are Stain free from BIORAD and the ladder is the Precision Plus All Protein ladder.

The analysis of the quantification was done by the same principle as the previous phosphorylation activity assay. We used as reference the time point 0 hours of the reaction containing PARP16 without kinase incubation and we normalized the values with the loading gel. A gradual increase of the activity of PARP16 can be seen by looking at the column graphs of figure 10. When PARP16 is previously incubated with the kinases, we can clearly see a change in its auto-ADP-ribosylation activity. These results then demonstrate that phosphorylation by kinases can intervene with and modify the activity of our target protein, PARP16. Comparing the quantification of the duplicates, it appears that phosphorylation tends to decrease the ADP-ribosylation activity of PARP16. However, the amounts of reduction of the activity by phosphorylation are not consistent.

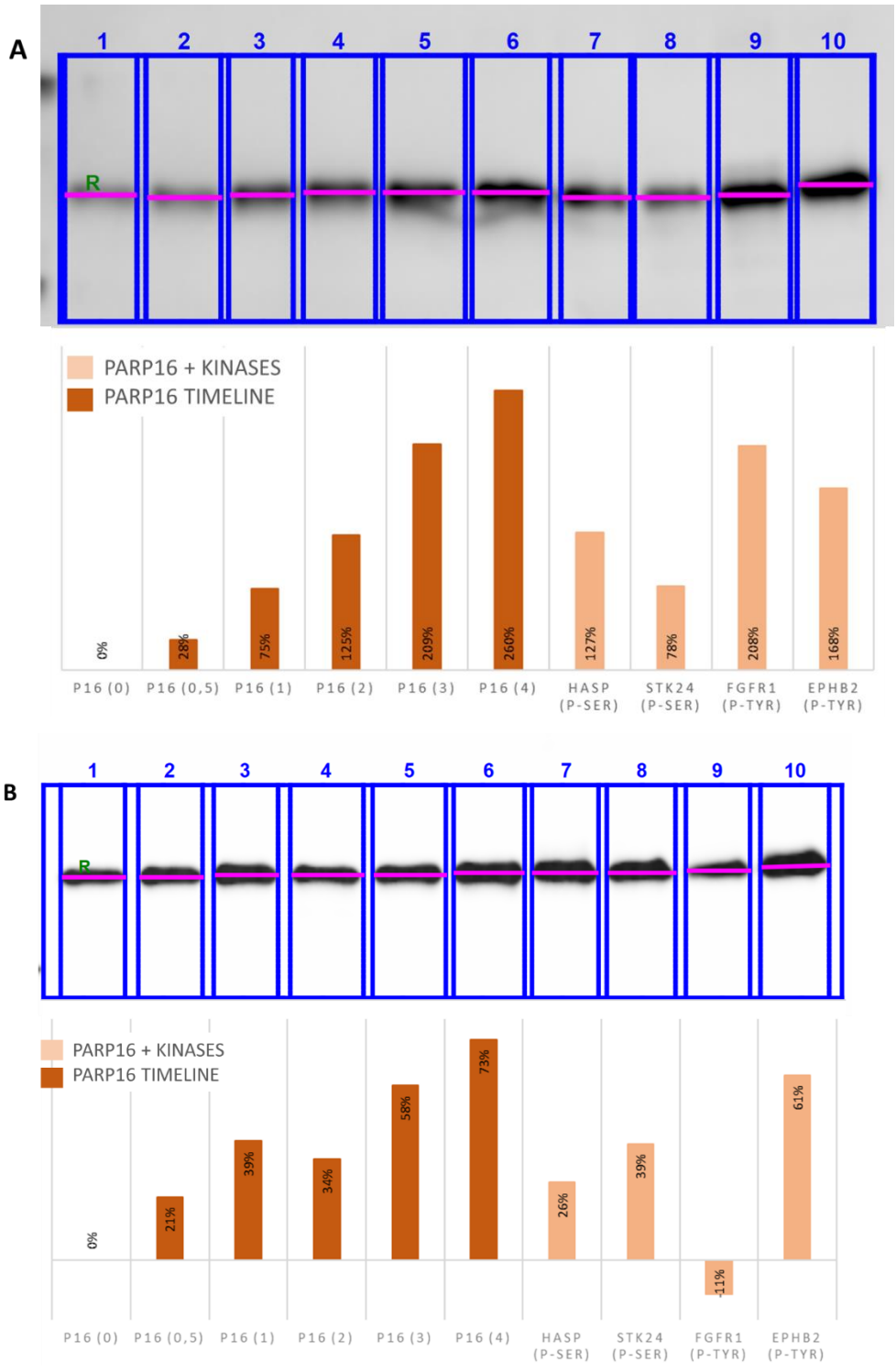

Figure 10: Quantification and normalization of the ADP-ribosylation of PARP16 without kinases over time and incubated with kinases at time point 4 hours. A) First assay quantification B) Second assay quantification.

4 Conclusions

In conclusion, we were able to co-transform and express 17 kinases. The purification protocol requires further optimization in order to obtain purified kinase samples without phosphatase contamination. However, the kinase activity tests showed positive results and suggested that the proteins displayed auto and trans phosphorylation activity. Also, we observed signs of previous phosphorylation in PARP16. These results were decisive for the activity assays of PARP16. Lastly, ADP-ribosylation activity tests with PARP16 indicate that the presence of phosphorylated residues by kinases in PARP16 have a direct effect in its activity. Phosphorylation, by any kinase, on our target protein led to a reduction of the activity in more than a 30% average. It is of great relevance PARP16 is a substrate of IRE1a and PERK in the UPR, and these proteins are, as previously mentioned, Ser/Thr-kinases [7]. These findings suggest that the ADP-ribosylation activity of PARP16 *in vivo* might be reduced as well. Therefore, further investigation in this field can be key for understanding this biological mechanism and how to modify it in order to understand better the UPR.

5 Future aspects

In pursuance of greater knowledge of this biological event it would be of interest to optimize protein expression and purification of the kinases. It would also be of use to repeat the auto and trans phosphorylation activity assays to obtain more conclusive results using a non-phosphorylated PARP16 sample. These assays would allow us to determinate the activity potential of the kinases and what residues are modified by them by mass spectrometry. It would be important to discover if the phosphorylation lies in the active site or on residues that are target for automodification. Unphosphorylated PARP16 may be obtained by incubation with phosphatases. Lastly, further experiments with IRE1a and PERK which are not included in the kinase library would be critical to address the biological reactions and mechanism occurring *in vivo*. We are already working on cloning and expression assays of those kinases.

6 References

[1] Di Paola S, Micaroni M, Di Tullio G, Buccione R, Di Girolamo M. PARP16/ARTD15 is a novel endoplasmic-reticulum-associated mono-ADP-ribosyltransferase that interacts with, and modifies karyopherin-ß1. PLoS One. 2012;7(6):e37352. doi: 10.1371/journal.pone.0037352. Epub 2012 Jun 11. PMID: 22701565; PMCID: PMC3372510.

[2] Hottiger MO, Hassa PO, Lüscher B, Schüler H, Koch-Nolte F. Toward a unified nomenclature for mammalian ADP-ribosyltransferases. Trends Biochem Sci. 2010 Apr;35(4):208-19. doi: 10.1016/j.tibs.2009.12.003. Epub 2010 Jan 26. PMID: 20106667.

[3] Cohen MS, Chang P. Insights into the biogenesis, function, and regulation of ADP-ribosylation. Nat Chem Biol. 2018 Feb 14;14(3):236-243. doi: 10.1038/nchembio.2568. PMID: 29443986; PMCID: PMC5922452.

[4] Aravind L, Zhang D, de Souza RF, Anand S, Iyer LM. The natural history of ADP-ribosyltransferases and the ADP-ribosylation system. Curr Top Microbiol Immunol. 2015;384:3-32. doi: 10.1007/82_2014_414. PMID: 25027823; PMCID: PMC6126934.

[5] Vyas S, Matic I, Uchima L, Rood J, Zaja R, Hay RT, Ahel I, Chang P. Family-wide analysis of poly(ADP-ribose) polymerase activity. Nat Commun. 2014 Jul 21;5:4426. doi: 10.1038/ncomms5426. PMID: 25043379; PMCID: PMC4123609.

[6] Leung AK, Vyas S, Rood JE, Bhutkar A, Sharp PA, Chang P. Poly(ADP-ribose) regulates stress responses and microRNA activity in the cytoplasm. Mol Cell. 2011 May 20;42(4):489-99. doi: 10.1016/j.molcel.2011.04.015. PMID: 21596313; PMCID: PMC3898460.

[7] Jwa M, Chang P. PARP16 is a tail-anchored endoplasmic reticulum protein required for the PERK- and IRE1α-mediated unfolded protein response. Nat Cell Biol. 2012 Nov;14(11):1223-30. doi: 10.1038/ncb2593. Epub 2012 Oct 28. Erratum in: Nat Cell Biol. 2013 Jan;15(1):123. PMID: 23103912; PMCID: PMC3494284.

[8] Hetz C, Zhang K, Kaufman RJ. Mechanisms, regulation and functions of the unfolded protein response. Nat Rev Mol Cell Biol. 2020 Aug;21(8):421-438. doi: 10.1038/s41580-020-0250-z. Epub 2020 May 26. PMID: 32457508; PMCID: PMC8867924.

[9] Albanese SK, Parton DL, Işık M, Rodríguez-Laureano L, Hanson SM, Behr JM, Gradia S, Jeans C, Levinson NM, Seeliger MA, Chodera JD. An Open Library of Human Kinase Domain Constructs for Automated Bacterial Expression. Biochemistry. 2018 Aug 7;57(31):4675-4689. doi: 10.1021/acs.biochem.7b01081. Epub 2018 Jul 26. PMID: 30004690; PMCID: PMC6081246.

[10] Wang S, Kaufman RJ. The impact of the unfolded protein response on human disease. J Cell Biol. 2012 Jun 25;197(7):857-67. doi: 10.1083/jcb.201110131. PMID: 22733998; PMCID: PMC3384412.

7 Appendix

PHOSPHATASES	MOLECULAR WEIGHT (Da)	COMPATIBLE KINASES	MOLECULAR WEIGHT (Da)
YopH	33445,79	FES	45357,90
		MERKT	36774,37
		EPHA3	41221,06
		EPHB2	36032,10
		FGFR3	37924,56
		SRC	35220,30
		ABL1	35730,67
		CSK	32600,42
		EPHB1	36293,42
		FGFR1	37694,21
Lambda	25218,77	KCC1G	33014,09
		KCC2D	32609,09
		HASP	41116,92
		STK24	33445,22
		CDK16	39070,72
		GAK	37134,28
		PMYT1	34259,84

Figure A1: Table of the molecular weight of the different phosphatases and kinases worked with.

STOCK CONCENTRATIONS	mg/ml	MW	nM	µM	mM
EPHA3	0,974	41221	23628,73	23,63	-
EPHB2	0,748	36032	20759,33	20,76	-
FGFR1	0,878	37694	23292,83	23,29	-
KCC2D	0,185	32609	5673,28	5,67	-
STK24	0,278	31500	8825,397	8,83	-
GAK	0,529	25800	20503,88	20,50	-
ATP (50x)	-	-	-	500000	500
EDTA (50x)	-	-	-	500000	500
MgCl2 (1/10)	-	-	-	100000	100
phosSTOP				unknown	unknown

Figure A2: Table of the stock concentrations from the different

10x reaction buffer A: 500mM HEPES 7.5, 1M NaCl, 10mM MgCl2, 1mM TCEP

BUFFER A REACTIONS		KINASE		ATP (1/100)		10x Buffer A	H2O	phosSTOP	Total volume
		µM	µl	µM	µl	µl	µl	µl	µl
A1	EPHA3	10	8,46	200	0,80	2,00	6,74	2,00	20,00
A2	EPHB2	10	9,63	200	0,80	2,00	5,57	2,00	20,00
A3	FGFR1	10	8,59	200	0,80	2,00	6,61	2,00	20,00
A4	KCC2D	4	14,10	200	0,80	2,00	1,10	2,00	20,00
A5	STK24	4	9,06	200	0,80	2,00	6,14	2,00	20,00
A6	GAK	10	9,75	200	0,80	2,00	5,45	2,00	20,00

10x reaction buffer B: 500mM Na2HPO4 pH 7.5, 1M NaCl, 1mM TCEP

BUFFER B REACTIONS		KINASE		ATP (1/100)		10x buffer B	H2O	MgCl2 (1/10)	phosSTOP	Total volume
		µM	µl	µM	µl	µl	µl	µl	µl	µl
B1	EPHA3	10	8,46	200	0,80	2,00	6,54	0,20	2,00	20,00
B2	EPHB2	10	9,63	200	0,80	2,00	5,37	0,20	2,00	20,00
B3	FGFR1	10	8,59	200	0,80	2,00	6,41	0,20	2,00	20,00
B4	KCC2D	4	14,10	200	0,80	2,00	0,90	0,20	2,00	20,00
B5	STK24	4	9,06	200	0,80	2,00	5,94	0,20	2,00	20,00
B6	GAK	10	9,75	200	0,80	2,00	5,25	0,20	2,00	20,00

Figure A3: Reaction set-up for the autophosphorylation assays.

STOCK CONCENTRATIONS	mg/ml	MW	nM	µM	mM
KCC1G	0,231	33014,09	6997,012	7,00	-
CDK16	0,334	39070,72	8548,601	8,55	-
HASP	0,199	41116,92	4839,857	4,84	-
PMTY1	0,477	41116,92	11601,06	11,60	-
KCC2D	0,185	32609	5673,28	5,67	-
STK24	0,278	31500	8825,397	8,83	-
GAK	0,529	25800	20503,88	20,50	-
ATP (50x)	-	-	-	500000	500
EDTA (50x)	-	-	-	500000	500
phosSTOP	-	-	-	unknown	unknown
PARP16	-	-	-	482	

Figure A4: Table of the stock concentrations from the different

ACTIVITY ON PARP16 OF SER/THR KINASES	KINASE		ATP (1/100)		EDTA (1/100)		10x Buffer A	H2O	PARP16		phosSTOP	Total volume
	µM	µl	µM	µl	µm	µl	µl	µl	µM	µl	µl	µl
KCC1G+PARP16+ATP	4	11,43	200	0,80	200	-	2	3,35	10	0,41	2	20
CDK16+PARP16+ATP	4	9,36	200	0,80	200	-	2	5,43	10	0,41	2	20
HASP+PARP16+ATP	3	12,40	200	0,80	200	-	2	2,39	10	0,41	2	20
PMTY1+PARP16+ATP	4	6,90	200	0,80	200	-	2	7,89	10	0,41	2	20
KCC2D+PARP16+ATP	4	14,10	200	0,80	200	-	2	0,68	10	0,41	2	20
STK24+PARP16+ATP	4	9,06	200	0,80	200	-	2	5,72	10	0,41	2	20
GAK+PARP16+ATP	4	3,90	200	0,80	200	-	2	10,88	10	0,41	2	20
KCC1G+PARP16+EDTA	4	11,43	200	-	200	0,80	2	3,35	10	0,41	2	20
CDK16+PARP16+EDTA	4	9,36	200	-	200	0,80	2	5,43	10	0,41	2	20
HASP+PARP16+EDTA	3	12,40	200	-	200	0,80	2	2,39	10	0,41	2	20
PMTY1+PARP16+EDTA	4	6,90	200	-	200	0,80	2	7,89	10	0,41	2	20
KCC2D+PARP16+EDTA	4	14,10	200	-	200	0,80	2	0,68	10	0,41	2	20
STK24+PARP16+EDTA	4	9,06	200	-	200	0,80	2	5,72	10	0,41	2	20
GAK+PARP16+EDTA	4	3,90	200	-	200	0,80	2	10,88	10	0,41	2	20
KCC1G+ ATP	4	11,43	200	0,80	200	-	2	5,35	10	-	2	20
CDK16+ ATP	4	9,36	200	0,80	200	-	2	25,43	10	-	2	20
HASP+ ATP	3	12,40	200	0,80	200	-	2	4,39	10	-	2	20
PMTY1+ ATP	4	6,90	200	0,80	200	-	2	9,89	10	-	2	20
KCC2D+ ATP	4	14,10	200	0,80	200	-	2	2,00	10	-	2	20
STK24+ ATP	4	9,06	200	0,80	200	-	2	7,72	10	-	2	20
GAK+ ATP	4	3,90	200	0,80	200	-	2	12,88	10	-	2	20
P16+ATP	-	-	200	4,00	200	-	10	73,93	10	2,07	10	100

Figure A5: Reaction set-up for the transphosphorylation assays.

STOCK CONCENTRATIONS	mg/ml	MW	nM	µM	mM
PARP16	-	-	482	-	-
HASP	0,199	41116,92	4839,856682	4,84	-
STK24	0,278	31500	8825,396825	8,83	-
EPHB2	0,748	36032	20759,32504	20,76	-
FGFR1	0,878	37694	23292,83175	23,29	-
NAD	-	-	-	10000,00	10
biotin-NAD	-	-	-	250,00	-
NAD-mix (10% biotin)	-	-	-	2000,00	2
phosSTOP	-	-	-	unknown	unknown
ATP (50x)	-	-	-	500000	500
MgCl2 (1/10)	-	-	-	100000	100

Figure A6: Table of the stock concentrations from the different

	PARP16 TIMELINE	PARP16		10x Buffer B	MgCl (1/100)	PHOSstop	H2O	control
		µM	µl	µl	µl	µl	µl	µl
1	PARP16 CONTROL	10	4,15	20,00	2,00	20,00	133,85	180,00

	PHOSPHORILATION	PARP16		KINASE		ATP (1/100)	10x Buffer B	MgCl (1/10)	PHOSstop	H2O	control
		µM	µl	µM	µl	µl	µl	µl	µl	µl	µl
2	PARP16 + HASP	10	0,41	3	12,40	0,80	2,00	0,20	2,00	0,19	18,00
3	PARP16 + STK24	10	0,41	4	9,06	0,80	2,00	0,20	2,00	3,52	18,00
4	PARP16 + FGFR1	10	0,41	4	3,85	0,80	2,00	0,20	2,00	8,73	18,00
5	PARP16 + EPHB2	10	0,41	4	3,43	0,80	2,00	0,20	2,00	9,15	18,00

	ADP-RIBOSYLATION	NAD-mix	
		µM	µl
1	PARP16 CONTROL	200	20,00
2	PARP16 + HASP	200	2,00
3	PARP16 + STK24	200	2,00
4	PARP16 + FGFR1	200	2,00
5	PARP16 + EPHB2	200	2,00

Figure A7: Reaction set-up for the ADP-ribosylation assays.